

An Integrated Network of Androgen Receptor, Polycomb, and TMPRSS2-ERG Gene Fusions in Prostate Cancer Progression

Jindan Yu,^{1,3,6,7} Jianjun Yu,^{1,3} Ram-Shankar Mani,^{1,3} Qi Cao,^{1,3} Chad J. Brenner,^{1,3} Xuhong Cao,^{1,2,3} Xiaoju Wang,^{1,3} Longtao Wu,⁷ James Li,^{1,3} Ming Hu,^{1,5} Yusong Gong,^{1,3} Hong Cheng,^{1,3} Bharathi Laxman,^{1,3} Adaikkalam Vellaichamy,^{1,3} Sunita Shankar,^{1,3} Yong Li,^{1,3} Saravana M. Dhanasekaran,^{1,3} Roger Morey,^{1,3} Terrence Barrette,^{1,3} Robert J. Lonigro,^{1,6} Scott A. Tomlins,^{1,3} Sooryanarayana Varambally,^{1,3,6} Zhaohui S. Qin,⁵ and Arul M. Chinnaiyan^{1,2,3,4,6,*}

¹Michigan Center for Translational Pathology

²Howard Hughes Medical Institute

³Department of Pathology

⁴Department of Urology

⁵Department of Biostatistics

⁶Comprehensive Cancer Center

University of Michigan Medical School, Ann Arbor, MI 48109, USA

⁷Division of Hematology/Oncology, Robert H. Lurie Comprehensive Cancer Center, Northwestern University, Feinberg Medical School, Chicago, IL 60611, USA

*Correspondence: arul@umich.edu

DOI 10.1016/j.ccr.2010.03.018

SUMMARY

Chromosomal rearrangements fusing the androgen-regulated gene *TMPRSS2* to the oncogenic ETS transcription factor *ERG* occur in approximately 50% of prostate cancers, but how the fusion products regulate prostate cancer remains unclear. Using chromatin immunoprecipitation coupled with massively parallel sequencing, we found that ERG disrupts androgen receptor (AR) signaling by inhibiting AR expression, binding to and inhibiting AR activity at gene-specific loci, and inducing repressive epigenetic programs via direct activation of the H3K27 methyltransferase EZH2, a Polycomb group protein. These findings provide a working model in which TMPRSS2-ERG plays a critical role in cancer progression by disrupting lineage-specific differentiation of the prostate and potentiating the EZH2-mediated dedifferentiation program.

INTRODUCTION

Prostate cancer is the most common non-skin cancer and a leading cause of cancer-related deaths in American men. We and others have previously characterized chromosomal rearrangements fusing the androgen-regulated gene *TMPRSS2* to ETS transcription factors such as *ERG* and *ETV1* in a majority of prostate cancers (Perner et al., 2006; Soller et al., 2006; Tomlins et al., 2005; Yoshimoto et al., 2006). Among these, fusions of *TMPRSS2* to the oncogenic ETS transcription factor *ERG* occur most frequently, accounting for 40%–80% of prostate cancers (Clark et al., 2007; Hermans et al., 2006). ERG has also been

implicated in recurrent gene fusions found in Ewing's sarcoma and acute myeloid leukemia (Hsu et al., 2004; Oikawa and Yamada, 2003). Knockdown of ERG in VCaP prostate cancer cells inhibits cell growth, cell invasion, and xenograft tumor growth (Tomlins et al., 2008; Wang et al., 2008). Overexpression of ERG increases cell invasion in vitro (Tomlins et al., 2008; Wang et al., 2008), and induces prostate cancer precursor-like lesions in mice (Klezovitch et al., 2008; Tomlins et al., 2008). Furthermore, ERG collaborates with genetic lesions of the PI3K pathway to promote prostate cancer progression in mouse models (Carver et al., 2009; King et al., 2009; Zong et al., 2009). Although it is clear that ERG may possess oncogenic properties, it has

Significance

Despite its high prevalence in prostate cancer, the TMPRSS2-ERG gene fusion was thought to merely represent one of many downstream mutations emanating from AR signaling. Here we mapped the genomic landscape of AR, ERG, and key histone modifications in prostate cancer. Although AR was found to activate genetic programs involved in prostate differentiation, we found that ERG binds to AR and a majority of AR target genes disrupting androgen signaling. In addition, ERG activates the PcG protein EZH2 facilitating a stem-cell-like dedifferentiation program. Thus, TMPRSS2-ERG plays a fundamental role in cancer by abrogating lineage-specific differentiation of the prostate. Furthermore, we provide a compendium of genome-wide location analyses related to AR and TMPRSS2-ERG that will be useful to the research community.

been much less clear as to how ERG promotes prostate cancer progression. Given the prevalence and recurrence of TMPRSS2-ERG in prostate cancer, we hypothesized that it plays an essential role in prostate tumorigenesis.

We have earlier demonstrated that ERG induces metalloproteinase and plasminogen activator pathway genes such as *MMP3*, *PLAT*, and *PLAU* (Tomlins et al., 2008). ERG is a member of the ETS family transcription factors that specifically bind to genomic regions containing the core GGA(A/T) motifs (Nye et al., 1992). Interestingly, ETS motifs were found enriched in the androgen receptor (AR) binding sites determined by chromatin immunoprecipitation (ChIP)-on-chip analysis and ETS1, another member of the ETS family transcription factors, was shown to physically interact with AR (Massie et al., 2007). Moreover, recent studies revealed that ERG represses the expression of the prostate-specific antigen (PSA) (Sun et al., 2008), while ETV1 induces PSA expression (Shin et al., 2009). The molecular crosstalk between ERG and AR, however, remains largely uncharacterized.

AR belongs to a family of nuclear transcription factors that mediate the action of steroid hormones. Cytoplasmic AR, when bound by androgen, translocates to the nucleus and binds to the 15-bp palindromic androgen response elements (ARE) on target genes (Heemers and Tindall, 2007). AR is paramount for the lineage-specific differentiation of the prostate, inducing the expression of prostate-specific genes such as *PSA* and *TMPRSS2*, and maintaining the differentiated prostate epithelial phenotype (Wright et al., 2003). Cellular dedifferentiation, by contrast, is a hallmark of malignant transformation. Previous studies have shown that a majority of metastatic prostate tumors have upregulated expression of the Polycomb group (PcG) protein EZH2, which plays critical roles in maintaining the undifferentiated state of embryonic stem (ES) cells via catalyzing H3K27 trimethylation (Lee et al., 2006; Varambally et al., 2002). EZH2 overexpression in advanced prostate cancer leads to epigenetic silencing of developmental regulators and tumor suppressor genes, subverting cancer cells to a stem-cell-like epigenetic state (Yu et al., 2007b).

Here we employed chromatin immunoprecipitation coupled with massively parallel sequencing (ChIP-Seq) (Barski et al., 2007; Johnson et al., 2007; Mikkelsen et al., 2007) to systematically map the genomic landscape of four transcription factors and eight histone marks across multiple prostate cancer cell lines as well as tissues (summarized in Table S1 available online). Integrative genomic analysis was undertaken to delineate the interactions among TMPRSS2-ERG, AR, and EZH2. In addition, we examined the mechanisms of TMPRSS2-ERG in prostate tumorigenesis in the context of AR-induced prostatic differentiation and EZH2-mediated cellular dedifferentiation.

RESULTS

Genomic Landscape of AR in Prostate Cancer

To determine AR binding sites across the human genome, we performed ChIP-Seq analysis of the LNCaP prostate cancer cells treated with either vehicle or saturating amounts of synthetic androgen R1881 as previously reported (Wang et al., 2007). To evaluate the reproducibility of the ChIP-Seq assay, we compared the distribution of sequencing reads mapped in

every 25 bp bin across the entire genome and observed substantial overlap between technical as well as biological replicates (Figure S1A). Using the HPeak program (<http://www.sph.umich.edu/csg/qin/HPeak/>), we identified enriched binding peaks from mappable sequencing reads. In LNCaP cells our study revealed 37,193 AR binding peaks, which include 82% of the AR-bound sites previously reported by ChIP-on-chip assay (Wang et al., 2009). Importantly, known AR binding sites, such as the enhancer upstream to the *FKBP5* gene, showed marked ChIP-Seq enrichment comprised of thousands of sequencing reads. By sorting the binding peaks by height, the top AR-bound genes included *FKBP5*, *C6ORF81*, *TACC2*, *CUTL2*, and *SLC43A1*, all of which showed “prostate-specific” expression based on the International Genomics Consortium’s expO microarray data set profiling 28 tumor types (www.oncoPrint.com) (Figure S1B). These genes also ranked among the top ten AR-bound genes in the VCaP prostate cancer cells that harbor the *TMPRSS2-ERG* gene fusions (Tomlins et al., 2005). Approximately 61% of the AR binding sites in the VCaP cells physically overlapped with those in LNCaP, suggesting shared as well as cell-type-specific AR recruitment (Figure 1A). The shared AR binding targets were further confirmed by the inclusion of previously reported androgen-sensitive 5′ partners of gene fusions in prostate cancer such as *TMPRSS2*, *SLC45A3*, and *C15ORF21* (Tomlins et al., 2007) (Figure S1C). By contrast, no AR binding was detected on the androgen-insensitive 5′ fusion partner gene *HNPRA2B1* that is constitutively active, supported by the enrichment of two markers of active transcription, histone H3 lysine 4 trimethylation (H3K4me3) and RNA polymerase II (RNA PolII), on its promoter. AR recruitment to these genetic loci was further confirmed by ChIP polymerase chain reaction (PCR) using gene-specific primers. Analysis of cell-type-specific AR binding revealed much higher false-negative rate of ChIP-Seq in VCaP than in LNCaP, partially accounting for the lesser amount of AR binding sites detected in the former (Figure S1D). We next examined the presence of consensus sequence motifs in the AR binding sites. Out of all 508 predefined motifs of vertebrate transcription factors (www.genomatix.de), the 15 bp canonical ARE, as expected, was the most enriched. In addition, the occurrence of the ARE motif was positively correlated with the height of ChIP-Seq binding peaks ($r = 0.87$, $p < 0.001$) and some binding peaks contained multiple AREs (Figure S1E). By categorizing all AR binding sites based on whether they contained a full or half or no ARE motifs, we found that the binding sites containing full ARE motifs had significantly ($p < 0.001$ by t test) higher enrichment peaks than those with half ARE motifs, which had higher peaks than those without any ARE motifs, supporting the role of ARE in recruiting AR. Furthermore, de novo motif search using the MEME program (Bailey and Elkan, 1994) identified a refined ARE motif that was markedly similar to the canonical ARE (Figure 1B). Surprisingly, the ETS family motifs were the second-most enriched motifs suggesting potential colocalization of ERG with AR (Table S2). Approximately 40% of all AR binding sites contained at least one ARE motif and about 29% contained an ETS motif, both being significantly ($p < 0.001$ by Fisher’s exact test) more than their respective occurrence in control sequences (Table S3).

To obtain a functional taxonomy of the AR-bound genes, we performed molecular concept map (MCM) analysis for

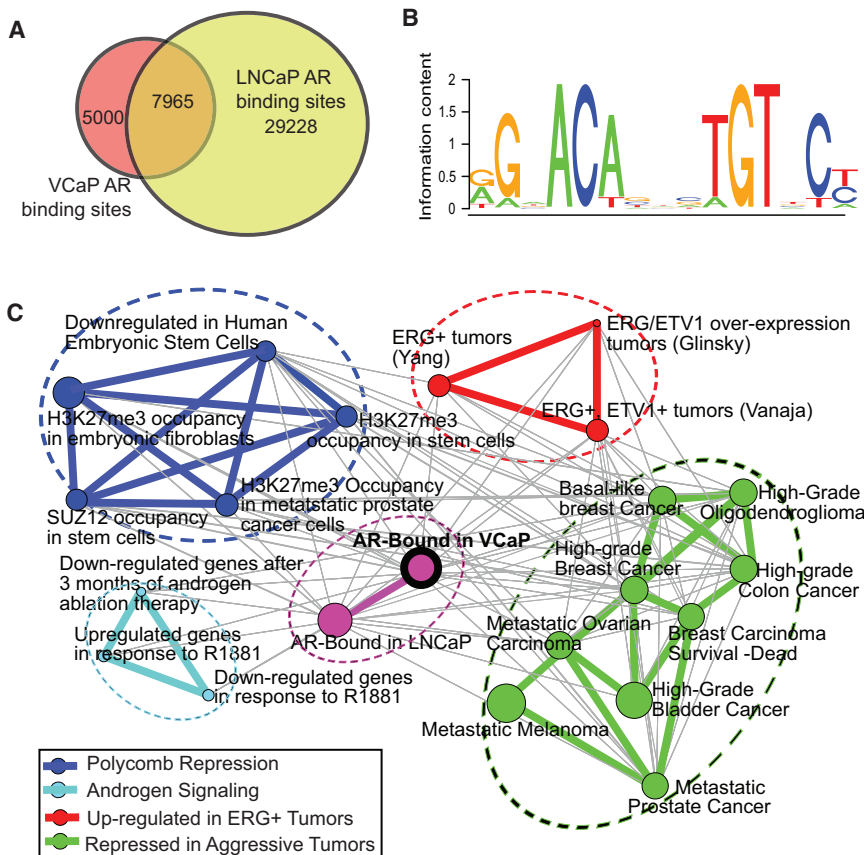


Figure 1. Genome-wide Location Analysis of AR in Prostate Cancer

(A) Venn diagram showing overlap of the ChIP-Seq AR binding sites in the LNCaP and VCaP prostate cancer cells.

(B) The consensus motif identified in the AR binding sites. De novo motif search was performed using the MEME program (Bailey and Elkan, 1994).

(C) An enrichment network linking AR, TMPRSS2-ERG pathways, and the polycomb-mediated dedifferentiation program. AR-bound genes (purple node with black ring) were derived by ChIP-Seq in the VCaP cells and analyzed by the MCM in OncoPrint. Each node represents one molecular concept or gene set with node size proportional to the number of genes. Each edge represents a statistically significant ($p < 1 \times 10^{-10}$) overlap of genes in the two linked nodes. Molecular concepts were grouped into five major clusters indicated by oval rings of distinct color. See also Figure S1 and Tables S1–S4.

enrichment of the AR-bound genes in thousands of pre-defined molecular concepts/gene sets in the OncoPrint database (www.oncoPrint.com). Out of approximately 20,000 molecular concepts, a total of 1,462 (7%) showed significant ($p < 0.001$) enrichment (Table S4). Not surprisingly, AR-bound genes in the VCaP cells significantly overlapped with those in the LNCaP cells ($p < 1.0 \times 10^{-100}$) and they both related to genes that are regulated by androgen in vitro or in vivo ($p < 1.0 \times 10^{-10}$) (Figure 1C). In addition, there was significantly enriched AR binding on “genes underexpressed in metastatic or high-grade tumors” ($p < 4.0 \times 10^{-15}$), confirming reduced androgen signaling in aggressive prostate tumors. Importantly, AR-bound genes were significantly enriched in a number of ERG-regulated gene sets ($p < 4.0 \times 10^{-13}$), indicating an interesting link between ERG regulation and androgen signaling. Notably, a group of most significantly enriched ($p < 1.0 \times 10^{-20}$) concepts related to stem cell gene signatures, including target genes of Polycomb group proteins and H3K27me3 in embryonic stem cells and metastatic prostate cancers (Boyer et al., 2006; Lee et al., 2006; Yu et al., 2007b), further connecting the AR and ERG pathways to PcG-mediated epigenetic silencing and cellular dedifferentiation.

ERG Occupancy of AR Target Genes in Prostate Cancer

To characterize the potential links among the transcriptional pathways of AR, ERG, and epigenetic modifications, we performed ChIP-Seq analysis of ERG and a number of key histone

marks in prostate cancer (Table S1). Approximately 42,000 ERG binding sites were identified in the VCaP cells including known ERG target genes such as *PLAU*, *PLAT*, *MMP3*, and *MMP9* (Tomlins et al., 2008) (Figure 2A). By contrast, only 608 binding sites were detected in the ERG-negative LNCaP cells. Interestingly, ChIP-Seq analysis of the RWPE benign prostate epithelial cells with stable ERG overexpression (RWPE+ERG) identified 6685 ERG binding sites, 58% of which overlapped with those detected in the VCaP cells (Figure 2B). Unlike AR, which was mostly enriched at distal enhancers, ERG primarily bound to the promoter regions of target genes (Figure 2C and Figure S2). Not surprisingly, the ETS family motifs were the most significantly enriched motifs in the ERG binding sites (Table S2) and MEME analysis discovered a de novo ERG motif that was strikingly similar to the consensus ETS motifs (Figure 2D).

To test the hypothesis that AR and ERG co-occupy target genes, we analyzed the overlap in their binding sites in every 25 bp bin across the entire genome. Although 61% of the AR-bound regions in the VCaP cells overlapped with those in LNCaP, approximately 44% of these sites, surprisingly, also recruited ERG (Figure 3A). This overlap between AR and ERG binding sites is remarkable, because AR and ERG each bound to only 0.1% and 0.7% sequences of the entire genome, respectively. To evaluate this overlap statistically, we compared AR and ERG binding sites with those of NRSF, a neural specific transcription factor that has not been associated with either AR or ERG (Johnson et al., 2007). Importantly, there was less than 2% of overlap. The overlap between the AR and ERG binding sites was significantly more than their overlap with NRSF ($p < 0.0001$ by Fisher’s exact test). Further, we compared the binding sites of AR and ERG with other transcription factors and epigenetic marks analyzed by ChIP-Seq in both LNCaP and VCaP cells (Figure S3A and Table S5). As expected, we observed

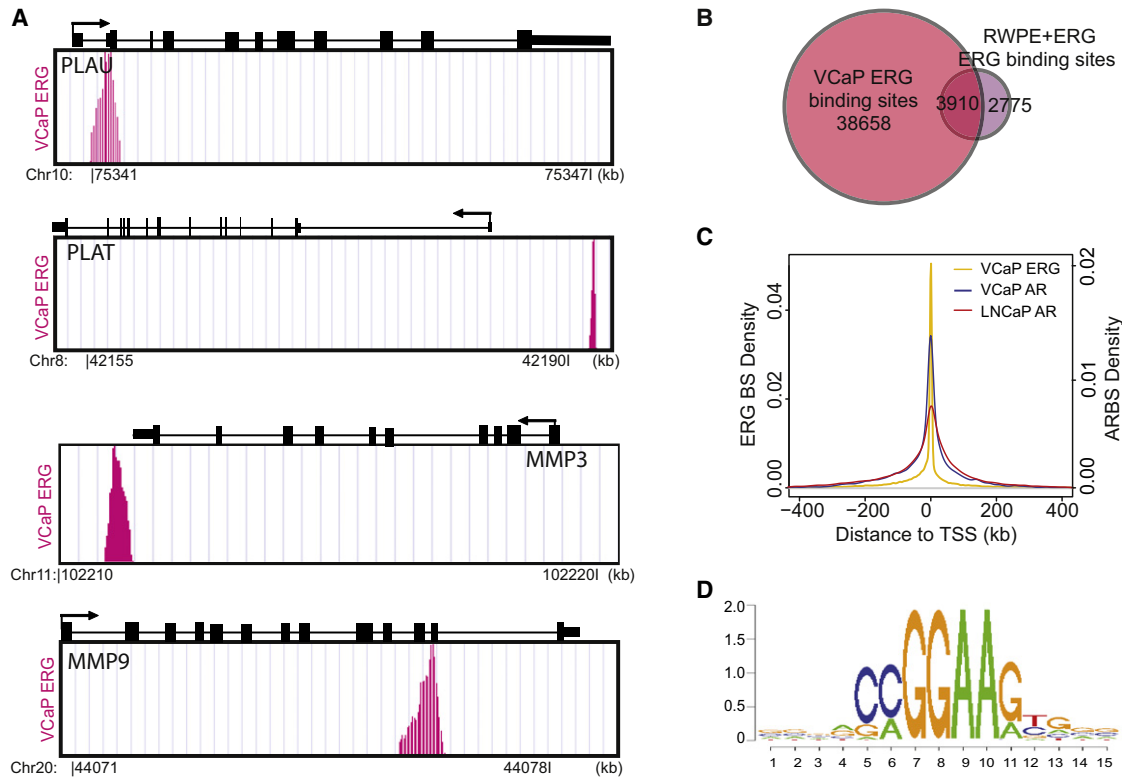


Figure 2. ChIP-Seq Analyses of ERG Binding Sites in Prostate Cancer

(A) ChIP-Seq analysis of the VCaP cells detected ERG binding to previously reported target genes (Tomlins et al., 2008).
 (B) Venn diagram showing overlap between the ERG binding sites identified in the VCaP cells and the RWPE+ERG cells. The RWPE cells were infected with lentivirus overexpressing ERG or lacZ and selected for stable clones. ChIP-Seq of ERG was performed in the stable RWPE+ERG cells using the RWPE+lacZ as control.
 (C) Distribution of AR or ERG binding sites relative to the transcriptional start sites (TSS) of all RefSeq genes. The y axis on the left and right represents the density of ERG (ERG BS) and AR binding sites (ARBS), respectively. See also Figure S2.
 (D) The consensus sequence motif identified in the ERG binding sites by the MEME program.

substantial overlap of the same factor across cell types. Remarkably, the overlap between AR and ERG in the VCaP cells was among the highest in all overlaps between different regulators, including those between AR and FoxA1, PolII, H3K4me1, H3K4me3, H3K9me3 and H3K27me3. The next strongest overlap was of AR with FoxA1 and Ace-H3, both of which have been previously reported (Jia et al., 2008; Lupien et al., 2008).

By assigning ChIP-Seq binding sites to their nearest genes, we found that ERG is in fact recruited to over 90% of the AR-bound genes (Figure 3B). This cobinding was further confirmed by re-ChIP-Seq experiment first using an antibody against ERG followed by an antibody against AR (Figure 3C). To further validate this, we randomly selected a set of five genes that bound both AR and ERG, including *NDRG1*, *C6orf81*, *CUTL2*, *LOC400451*, and *ZBTB16* (Figure 3D and Figure S3B). Importantly, using gene-specific primers, we confirmed AR and ERG co-occupancy on all selected genes by conventional ChIP-PCR assays (Figure 3E). In addition, the expression of these genes was found to be differentially regulated by both androgen stimulation and ERG RNA interference (Figure S3C).

To confirm the interconnected pathways of ERG and AR in vivo, we performed ChIP-Seq analysis of a human prostate tumor that expressed both ERG and AR, and identified 6,967 ERG and

12,036 AR binding sites, respectively. Not surprisingly, they both overlapped significantly with their respective binding sites identified in prostate cancer cell lines ($p < 0.001$ by Fisher's exact test). Importantly, a comparison of the AR- and ERG-binding sites in the prostate tumor specimen revealed a remarkable overlap (44%) that is comparable to that (43.97%) observed in the VCaP cell line model (Figure 3F). MCM analysis of the 1534 tissue ERG-bound genes revealed a core transcriptional regulatory circuitry composed of biological correlates with highly significant overlaps ($p < 1.0 \times 10^{-90}$); these include ERG-bound and AR-bound genes in tumors, ERG-bound and AR-bound genes in the VCaP cells, AR-bound genes in the LNCaP cells, and ERG-bound genes in the stable RWPE+ERG cells (Figure S3D).

Next, we determined if ERG and AR physically interact. Coimmunoprecipitation assays demonstrated an endogenous interaction between the AR and ERG proteins in cell line as well as prostate cancer tissues (Figure 3G and Figure S3E). Using ethidium bromide preincubation to deplete DNA, we demonstrated that the interaction between AR and ERG was DNA independent. Further, in vitro protein-protein interaction assays revealed that AR directly bound to the ETS domain of the ERG protein (Figure 3H and Figure S3F). This interaction was further pinpointed to the C-terminal half (ETS-3) of the ETS domain.

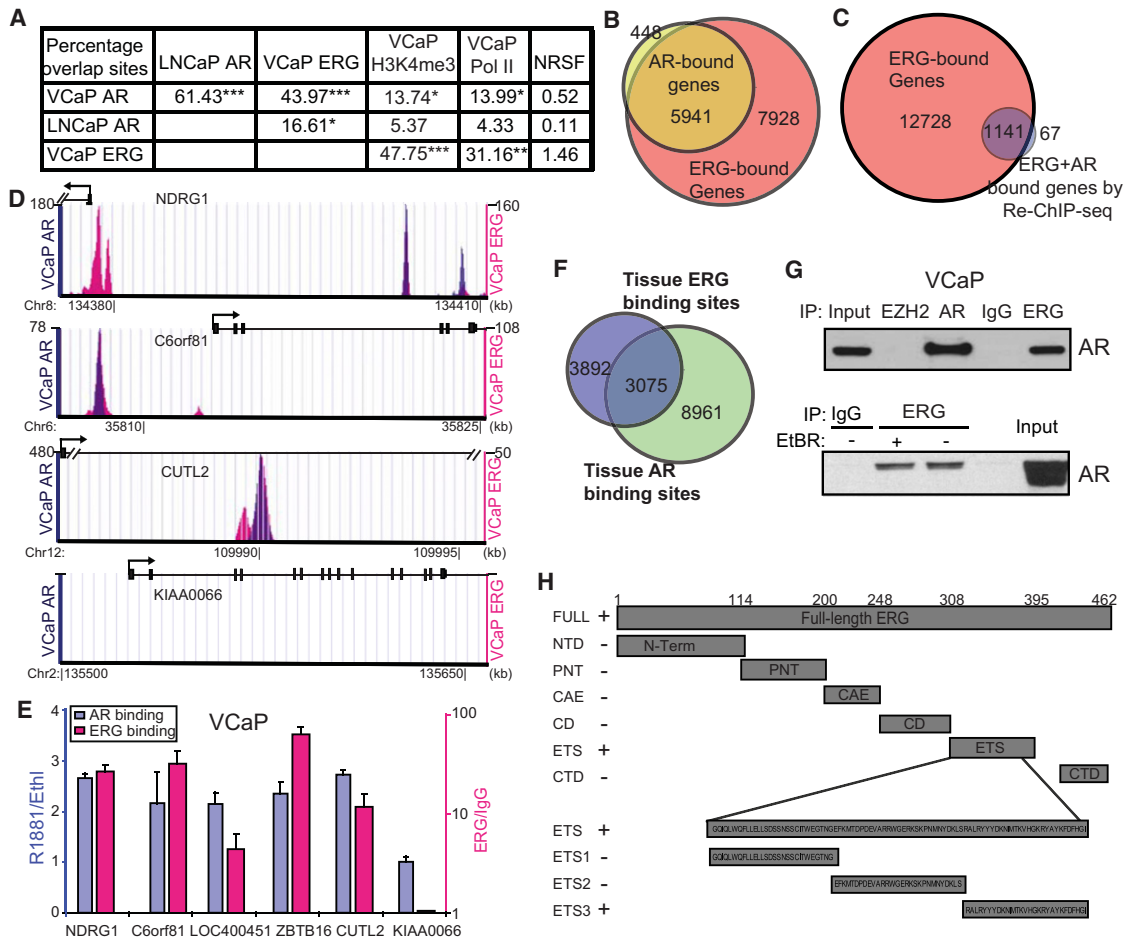


Figure 3. ERG and AR Co-occupancy of Target Genes in Prostate Cancer

(A) Overlap between the binding sites of different regulators. Significance of overlap was measured relative to their respective overlap with the NRSF binding sites. * $p < 0.05$, ** $p < 0.01$, and *** $p < 0.001$ by hypergeometric test.

(B) ERG binds to a majority of the AR-bound genes. AR or ERG ChIP-Seq binding sites were each assigned to the nearest gene on the genome to derive the list of bound genes.

(C) Overlap between the ERG-bound genes and the genes that are bound by both AR and ERG as determined by re-ChIP-Seq using an anti-ERG and an anti-AR antibody.

(D) Representative genes co-occupied by AR and ERG. On the y axes are the number of reads of AR (left, in blue) and ERG (right, in red) binding sites. Above the plot are the TSS and direction denoted by arrows, exons by black box, and introns by horizontal lines, respectively. The genomic coordinates are indicated below the plot.

(E) ChIP-PCR confirms AR and ERG co-occupancy on selected genes. The y axis on the left represents AR ChIP enrichment in VCaP cells treated with R1881 normalized to the ethanol (Ethl) treated cells. The y axis on the right represents ChIP enrichment (in log scale) by an anti-ERG antibody normalized to IgG. Error bars represent $n = 3$, mean and standard error of the mean (SEM). The 3' intronic region of the *KIAA0066* gene was used as a negative control.

(F) AR and ERG co-occupancy in a prostate cancer tissue. A prostate tumor tissue that expresses both AR and *TMPRSS2-ERG* were analyzed by ChIP-Seq.

(G) Physical interaction between the AR and ERG proteins. VCaP cells were immunoprecipitated by various antibodies and immunoblotted for AR. To deplete DNA, VCaP cell lysates were preincubated with ethidium bromide for 30 min before immunoprecipitation. Representative experiment of four independent co-immunoprecipitation assessments is shown.

(H) Interaction of ERG with AR in vitro via the ETS domain. HaloTag-ERG protein and mutants were generated by in vitro transcription/translation in wheat germ extracts. Recombinant GST-AR was incubated with the in vitro translated protein products and glutathione beads used in pull-down assays. The interaction between AR and various domains of ERG are summarized and indicated as + or -. See also Figure S3 and Table S5.

The *TMPRSS2-ERG* Gene Fusion Product Disrupts Androgen Signaling

Interestingly, one of the top genomic loci bound by ERG was the promoter of the *AR* gene as illustrated by ChIP-Seq and confirmed by ChIP-PCR (Figures 4A and 4B). By overexpressing ERG we observed significantly decreased *AR* transcript in multiple prostate cell lines, including the VCaP and LNCaP pros-

tate cancer cells and the immortalized RWPE prostate epithelial cells (Figure 4C). Concordantly, knockdown of ERG in VCaP cells led to *AR* upregulation, further supporting an inhibitory role of ERG on the *AR* gene (Figures S4A and S4B). In addition, we observed a marked decrease of AR protein following ERG overexpression in the LNCaP and VCaP prostate cancer cells as well as in the 22RV1 cells that are free of ETS family gene fusions,

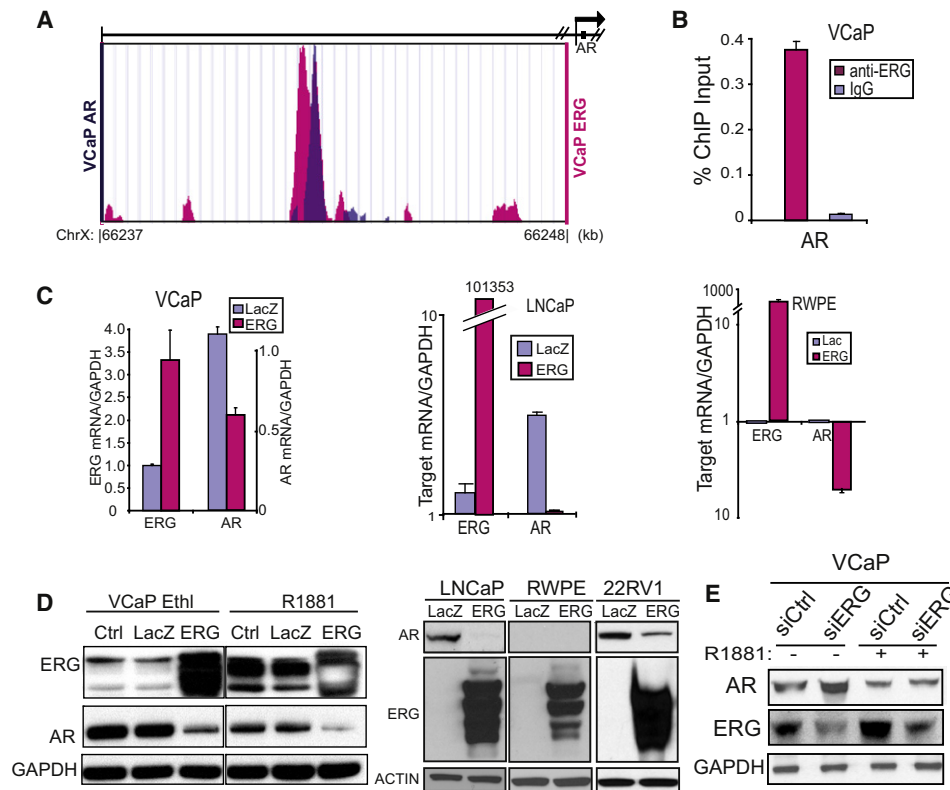


Figure 4. ERG Negatively Regulates the AR Gene

(A) ChIP-Seq showing AR and ERG cobinding to the regulatory regions of the AR gene. The y axes are as denoted as in Figure 3D.

(B) ChIP-PCR confirms ERG binding to the AR promoter. Error bars represent n = 3, mean ± SEM.

(C) Ectopic ERG overexpression represses the AR transcript. VCaP and LNCaP prostate cancer cells and RWPE benign prostate epithelial cells were infected by LacZ or ERG adenovirus. QRT-PCR was used to assay the ERG and AR transcript normalized to GAPDH. Error bars represent n = 3, mean ± SEM.

(D) ERG represses the AR protein. VCaP (in the presence or absence of androgen R1881), LNCaP, RWPE, and 22RV1 cells were infected with ERG for 48 hr before immunoblotting.

(E) ERG knockdown derepresses the AR protein. RNA interference of ERG was done in VCaP cells in the presence or absence of androgen. See also Figure S4.

whereas AR protein was expectedly not detected in the RWPE cells (Figure 4D and Figure S4C). Consistent with this, RNA interference of ERG in the hormone-starved VCaP cells greatly increased AR protein (Figure 4E). Adding androgen to these cells dramatically increased ERG expression, as expected. AR levels, however, were decreased, further demonstrating a negative regulation. Moreover, we showed that ERG overexpression greatly reduced AR promoter reporter activity in LNCaP cells (Figure S4D). In addition, AR and ERG expression were significantly anticorrelated ($r = -0.35$, $p = 0.001$) in vivo in localized prostate tumors (Figure S4E).

Besides directly regulating AR itself, ERG was recruited to a majority of AR target genes at gene-specific loci, for instance *KLK3*, *KLK2*, *SLC45A3*, and *FKBP5* (Figure 5A). We thus analyzed AR target gene expression in 67 localized prostate tumors that were classified into either ERG-positive (ERG+) or ETS-negative (ETS-) depending on the status of ETS family gene fusions. ETS- tumors were used as a negative control for comparison so as to preclude any effects from non-ERG ETS family gene fusions. Importantly, GSEA analysis demonstrated significant enrichment ($p < 0.001$) of “genes induced by androgen” in the gene set that is “repressed in ERG+ relative to ETS- pros-

tate tumors,” thus linking androgen induction with ERG repression (Figure 5B). For example, *KLK3*, *TMPRSS2*, *KLK2*, and *KLK4* were all expressed at significantly lower levels in the ERG+ than the ETS- prostate tumors (Figure S5A). This is an interesting finding that is consistent with our overall hypothesis that ERG functions to repress androgen regulation of a lineage-specific differentiation program. To further confirm this, we overexpressed ERG in LNCaP cells and carried out quantitative reverse-transcription polymerase chain reaction (qRT-PCR) analysis of a set of known androgen-induced genes, many of which are markers of prostate epithelial differentiation. Importantly, our results showed marked inhibition of these genes, while ERG expectedly activated other targets such as *PLAT* and *PLAU* (Tomlins et al., 2008) (Figure 5C). Similar suppression of androgen signaling by ERG was also observed in the 22RV1 cells that are negative for ETS family gene fusions (Figure S5B). We next investigated whether RNA interference of ERG may rescue this inhibition using the TMPRSS2-ERG-positive VCaP cells. We first treated hormone-starved VCaP cells with androgen and confirmed androgen-induced expression of AR target genes. Remarkably, the expression of these genes can be further increased by RNA interference of ERG, confirming endogenous

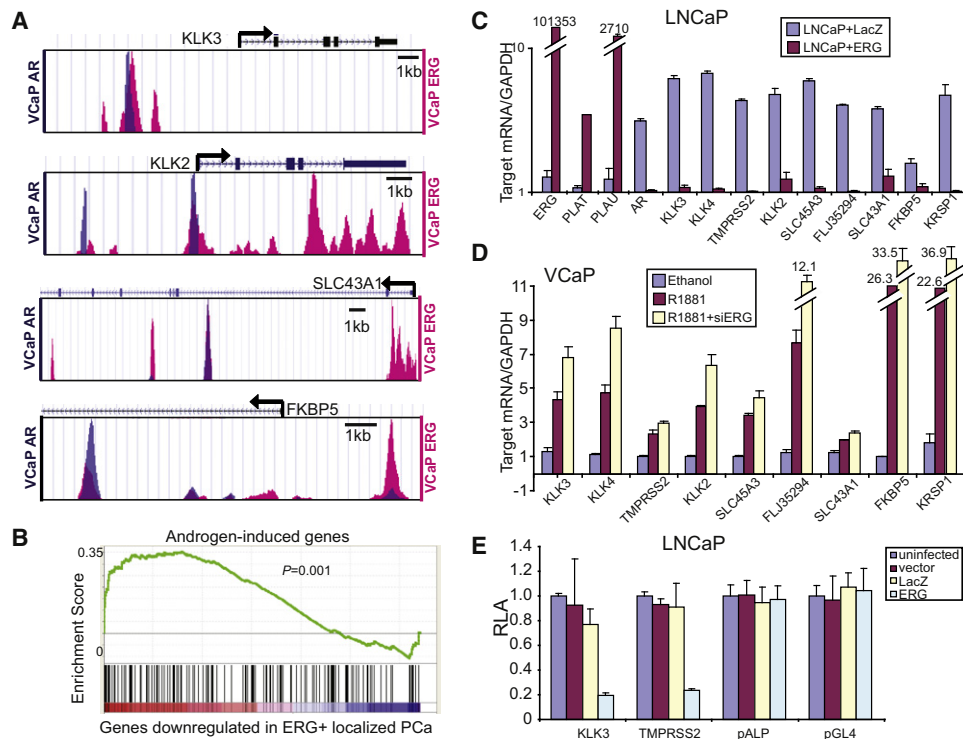


Figure 5. ERG Attenuates AR Transcriptional Activity

(A) ChIP-Seq showing AR and ERG cobinding to the regulatory regions of representative AR target genes. The y axes are as denoted in Figure 3D. (B) Androgen-induced genes are significantly enriched for repression by ERG. Androgen-induced genes were obtained from microarray analysis of time-course androgen treatment of LNCaP cells. ERG-repressed genes are downregulated in the ERG+ (n = 35) relative to the ETS- (n = 31) prostate tumors based on cancer gene expression microarray profiling. (C) ERG overexpression represses AR target genes. LNCaP cells were infected with ERG or lacZ for 48 hr prior to qRT-PCR analysis. *ERG*, *PLAT*, and *PLAUI* were used as positive controls for ERG overexpression. (D) ERG knockdown derepresses androgen-induced genes. VCaP cells were hormone starved for 2 days and treated with ethanol, synthetic androgen R1881, or R1881 with concurrent RNA interference targeting ERG for 48 hr before qRT-PCR analysis. The level of ERG knockdown is shown in Figure S4B. (E) Suppression of the *KLK3* and *TMPRSS2* promoters by ERG. LNCaP cells were cotransfected with various promoter reporter constructs along with pRL-TK (the internal control) at 24 hr postinfection of ERG or LacZ, incubated for another 24 hr, and then monitored for luciferase activity. Error bars represent n = 3, mean ± SEM. See also Figure S5.

ERG suppression of androgen response in the VCaP cells that can be derepressed by removing ERG (Figure 5D).

ChIP-PCR analysis of LNCaP cells following ERG titration revealed gradually increased ERG binding, but decreased AR binding, on these gene-specific genomic loci, supporting direct regulation by ERG independent of AR (Figures S5C and S5D). Consistent with this, ChIP-Seq analysis of VCaP cells following RNA interference of ERG revealed a 24% decrease in the number of ERG binding sites and a 26% increase in AR binding sites. Further, ERG overexpression in cells with either AR knockdown or AR overexpression continued to inhibit AR target genes (Figures S5E and S5F). Furthermore, luciferase reporter assays demonstrated substantially reduced (~5-fold) promoter activities of the *KLK3* and *TMPRSS2* gene by ERG overexpression (Figure 5E). Therefore, ERG disrupts androgen signaling through multiple mechanisms including by inhibiting AR expression, binding to and repressing AR downstream targets at gene-specific loci.

We next examined the oncogenic role of *TMPRSS2-ERG* gene fusions in the context of androgen signaling. Interestingly, ectopic overexpression of ERG in VCaP and LNCaP prostate

cancer cells remarkably increased cell invasion in the presence or absence of androgen, independent of AR (Figures 6A and 6B). Similarly, ERG overexpression dramatically induced cell proliferation, independent of androgen as well as AR protein expression (Figures 6C–6E). We therefore tested if ERG is able to drive androgen-independent prostate cancer cell growth. Stable clones of VCaP cells expressing *ERG* (VCaP+ERG) or the *GUS* control gene (VCaP+GUS) were selected and assayed for cell proliferation. Remarkably, we observed that the VCaP+ERG cells grow significantly faster than the VCaP+GUS cells (Figure 6F). In addition, the VCaP+ERG cells were able to continuously proliferate in the absence of androgen, while the VCaP+GUS cells failed to grow (Figure 6G). Therefore, by inhibiting AR-mediated prodifferentiation and regulating AR-independent oncogenesis *TMPRSS2-ERG* may provide a potential mechanism for androgen resistance.

***TMPRSS2-ERG* Induces EZH2-Mediated Epigenetic Silencing**

By MCM analysis we have earlier shown a link of ERG and androgen signaling with Polycomb-mediated H3K27

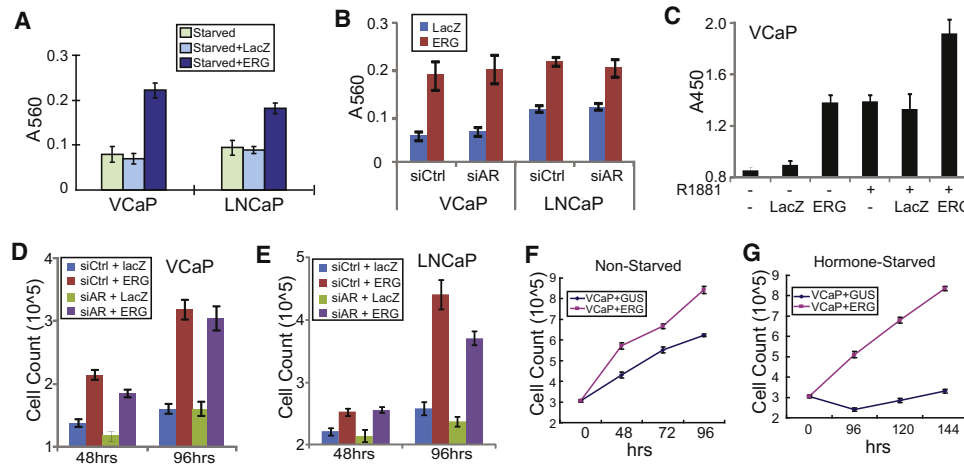


Figure 6. ERG Regulates the Neoplastic Properties of Prostate Cancer Cells Independent of Androgen Signaling

(A) Ectopic ERG overexpression induces prostate cancer cell invasion in the absence of androgen. The VCaP and LNCaP prostate cancer were hormone-starved for 1 day, and infected with ERG or control for another 2 days in the absence of androgen.
 (B) Ectopic ERG overexpression induces prostate cancer cell invasion independent of AR. VCaP and LNCaP cells were subjected to RNA interference against AR or control for 1 day before adenovirus infection of ERG or LacZ.
 (C) Ectopic ERG overexpression induces VCaP cell growth independent of androgen. VCaP cells were hormone deprived for 48 hr before infection with LacZ or ERG adenovirus in the presence or absence of androgen.
 (D, E) Ectopic ERG overexpression induces prostate cancer cell growth independent of AR expression. VCaP and LNCaP cells were subjected to RNA interference targeting AR or control for 1 day before adenovirus infection by ERG or LacZ. Cell proliferation was assayed at 48 hr or 96 hr after infection.
 (F) Ectopic ERG overexpression in prostate cancer cells increases cell growth. VCaP cells were infected with lentivirus expressing ERG or GUS (control). Stable clones expressing ERG (VCaP+ERG) or control (VCaP+GUS) were plated equally, and assayed for cell proliferation in regular medium.
 (G) Ectopic ERG overexpression confers cell growth in the absence of AR signaling. Equal numbers of stable VCaP+ERG and control cells were hormone-deprived for 48 hr and assayed for cell proliferation in hormone-deprived medium.
 Error bars represent $n = 3$, mean \pm SEM.

methylation, which has been shown to prevent the differentiation of embryonic stem cells and contribute to tumor cell dedifferentiation (Boyer et al., 2006; Lee et al., 2006; Yu et al., 2007b) (Figure 1C). We thus hypothesized that, besides inhibiting AR-mediated prodifferentiation, ERG may potentiate pathways involving H3K27me3 to control cell dedifferentiation. Indeed, whereas AR and H3K27me3 binding sites rarely overlap (<2%) in LNCaP, there was substantially more overlap (13%) in VCaP, probably due to the recruitment by ERG (Figures S6A and S6B). To test this, we investigated ERG regulation of the H3K27 methyltransferase EZH2. Interestingly, ChIP-Seq analysis revealed ERG binding to the *EZH2* promoter, which was confirmed by ChIP-PCR (Figures 7A and 7B). In addition, RNA interference of ERG greatly decreased EZH2 expression (Figure 7C). Concordant with this, ERG overexpression in LNCaP and RWPE cells markedly induced EZH2 (Figure 7D). Further, *EZH2* and *ERG* expression were positively correlated ($r = 0.23$, $p = 0.043$) in clinically localized prostate tumors. *EZH2* expression was significantly higher ($p < 0.001$) in the ERG+ ($n = 35$) than the ETS- ($n = 31$) tumors, thus supporting a model in which ERG activates EZH2 (Figure 7E).

We next investigated if ERG regulates EZH2-mediated epigenetic silencing. ChIP-Seq analysis demonstrated ERG binding to a number of previously reported EZH2 target genes such as *ADRB2*, *CDH1*, *DAB2IP*, *SNCA*, and *SOCS* (Cao et al., 2008; Chen et al., 2005; Yu et al., 2007b) (Figure S6B). Remarkably, whereas ERG activated *EZH2* expression, it strongly repressed

the expression of EZH2 target genes, thus supporting ERG activation of EZH2-mediated epigenetic silencing in prostate cancer (Figure 7F and Figure S6C). In addition, silencing of EZH2 restored the expression of EZH2 target genes such as *DAB2IP*, loss of which was recently shown leading to epithelial-to-mesenchymal transition and cellular maldifferentiation (Figure S6D) (Min et al., 2010; Xie et al., 2010). To further test a genome-wide association between ERG and EZH2-mediated dedifferentiation pathways, we investigated whether the expression pattern of PcG target genes are able to predict the status of TMPRSS2-ERG gene fusions in prostate tumors. We first derived previously reported Polycomb gene signatures associated with ESCs and poorly differentiated tumors, including target genes of Polycomb repressive complex 2 (PRC2), of PcG proteins SUZ12 and EED, and of H3K27me3 (Ben-Porath et al., 2008). We then analyzed the power of these gene signatures in predicting the status of TMPRSS2-ERG gene fusions in clinically localized prostate tumors. Importantly, the expression pattern of all PcG-related gene signatures accurately predicted the ERG status, whereas irrelevant control gene sets, including the target genes of histone H3, PolII, H3K36me3, and H3K4me3, were significantly ($p < 0.001$) less predictive (Figure 7G). Notably, androgen-induced genes (presumably repressed by ERG) also successfully predicted ERG status in prostate tumors. Therefore, ERG may have more global effects by disrupting androgen-mediated prostatic differentiation and inducing EZH2-mediated cellular dedifferentiation (Figure 7H).

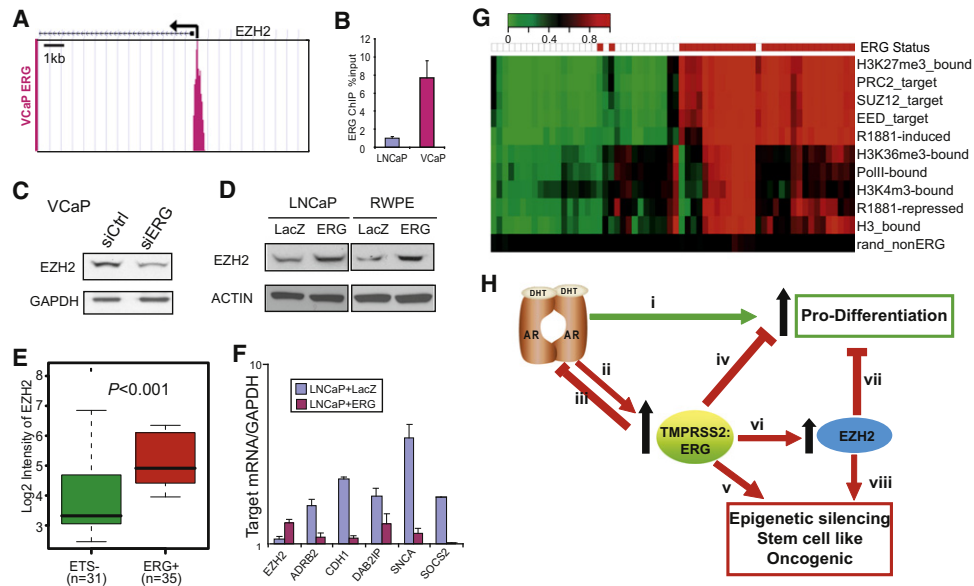


Figure 7. ERG Induces EZH2-Mediated Epigenetic Silencing

(A, B) ChIP-Seq and ChIP-PCR shows ERG binding to the *EZH2* promoter in VCaP cells. Error bars represent $n = 3$, mean \pm SEM.

(C) ERG knockdown in VCaP cells decreases EZH2 protein.

(D) ERG overexpression increases EZH2 protein. LNCaP and RWPE cells were infected with ERG or LacZ adenovirus for 48 hr before immunoblot analysis.

(E) *EZH2* is expressed at significantly ($p < 0.001$) higher levels in the ERG+ ($n = 35$) than the ETS- ($n = 31$) prostate tumors.

(F) ERG overexpression in the LNCaP cells activates EZH2 and represses known EZH2 target genes. LNCaP cells were infected with LacZ or ERG adenovirus for 48 hr and analyzed by qRT-PCR. Error bars represent $n = 3$, mean \pm SEM. See also Figure S6.

(G) Polycomb-related signatures and androgen-induced genes predict the status of *TMPRSS2-ERG* gene fusion in localized prostate tumors. The target genes of PcG proteins in embryonic stem cells were derived from a previous study (Ben-Porath et al., 2008), while the control gene signatures were taken from the ChIP-Seq experiments. Androgen-induced or androgen-repressed genes were from microarray profiling of the LNCaP cells following androgen treatment. A random signature not related to ERG (by removing ERG-regulated genes) was used as an absolute negative control (rand_nonERG). The Polycomb signatures and the androgen-induced genes have prediction scores significantly ($p < 0.001$) better than the other gene sets.

(H) A model of *TMPRSS2-ERG* in prostate cancer by disrupting prostate-specific differentiation and potentiating a stem-cell-like dedifferentiation program. (i) androgen signaling leads to normal prostate differentiation. (ii) Formation of the *TMPRSS2-ERG* somatic mutation. (iii) Inhibition of AR expression and direct interaction with AR by the *TMPRSS2-ERG* fusion product. (iv) ERG binding to AR target gene loci for negative regulation. (v and vii) Activation of epigenetic silencing, stem-cell-like state, and oncogenesis. (vi) Induction of EZH2. (vii) Induction of H3K27 marks and epigenetic silencing of pro-differentiation genes.

DISCUSSION

In the present study, we systematically mapped the genomic landscape of AR, ERG, FoxA1, and RNA PolII, along with eight critical histone marks in multiple prostate cancer cell lines as well as in one prostate tumor specimen. These studies not only reveal important biological findings regarding the mechanisms of *TMPRSS2-ERG* gene fusions in prostate cancer, but they also provide a compendium of 57 genome-wide ChIP-Seq experiments and a large set of paired microarray expression profiling data that will be useful for the investigation of biological mechanisms of cancer and steroid hormone receptor signaling.

By analyzing these genome-wide maps, we provide a working model of how *TMPRSS2-ERG* gene fusions regulate prostate cancer progression. In the context of an androgen-regulated gene fusion such as *TMPRSS2-ERG*, this fusion product can attenuate androgen signaling by multiple, cooperative mechanisms including direct inhibition of AR expression and attenuation of AR signaling at gene-specific loci (Figure 7H). Furthermore, our study reveals an additional pathway of ERG in perturbing cell differentiation through the Polycomb group proteins. Enrichment of H3K27me3-marked genes silenced in

ESCs and aggressive tumors was first apparent by MCM analysis of AR-occupied genes in prostate cancer, linking both AR and ERG to repressive epigenetic signatures (Figure 1C). This was further substantiated in prostate cancer tissues harboring *ERG* gene fusions being distinguishable by H3K27me3-containing and/or Polycomb-occupied genes. ERG was found to be a direct activator of EZH2 and the level of EZH2 expression was associated with the ERG status in a cohort of prostate tumors (Figure 7). Thus, *TMPRSS2-ERG* plays a central role as a “malignant regulatory switch” that shuts down androgen signaling, inhibiting normal prostate differentiation and turning on EZH2 expression, which induces an ESC-like dedifferentiation program.

Because *TMPRSS2-ERG* gene fusions are androgen-responsive, they were thought to merely represent one of many mutated pathways emanating from AR signaling. Our results, however, suggest that *TMPRSS2-ERG* plays a much more fundamental role. As an early-onset genetic lesion, *TMPRSS2-ERG* gene fusion may provide a mechanism for AR overexpression and mutation in advanced prostate cancer. Antiandrogen treatments such as bicalutamide (also called Casodex) or flutamide are currently being used to treat advanced disease (Anderson,

2003). Unfortunately, patients treated with these AR antagonists often develop recurrent disease that is resistant to this therapy. Tumors from men with castration-resistant metastatic prostate cancer (CRMPC) often overexpress AR through multiple mechanisms including AR amplification (Scher and Sawyers, 2005). Repression of AR by *TMPRSS2-ERG* may provide a malignant selection pressure contributing to recurrent tumors with AR amplification. This is supported by our observation of a negative correlation ($r = -0.35$, $p = 0.0014$) between AR and ERG expression in localized prostate tumors, but a positive correlation ($r = 0.30$, $p = 0.058$) in metastatic prostate cancers. Further, whereas AR amplification on its own is not sufficient to induce hyperplastic lesions, overexpression of a CMV-promoter driven AR (thus not susceptible to ERG repression, mimicking a hormone-refractory state with AR amplification), together with forced ERG overexpression, has recently been shown to promote the development of a more poorly differentiated, invasive adenocarcinoma (Zong et al., 2009). This may also suggest that therapies targeting AR may not produce a durable response in prostate cancer patients when the underlying mutation may in fact be *TMPRSS2-ERG*. Paradoxically, therapies employing high-dose testosterone may have a beneficial effect transiently by favoring a normal differentiation state. Consistent with this, preclinical models suggest that high doses of exogenous testosterone inhibit prostate cancer growth while low levels of testosterone promote tumor growth (Koivisto et al., 1997; Kokontis et al., 1998). Recently, high doses of exogenous testosterone have been shown to be safe in patients with CRMPC (Morris et al., 2009). Bicalutamide and flutamide exhibit a partial agonistic effect that may also promote normal prostate differentiation, which is eventually overcome by *TMPRSS2-ERG* expression and consequent resistant disease.

Taken together, our findings provide a working model in which *TMPRSS2-ERG* plays a critical role in cancer progression by disrupting the AR lineage-specific differentiation program of the prostate and favoring EZH2-mediated cellular dedifferentiation. In addition, by inhibiting AR signaling, *TMPRSS2-ERG* may exert a selective pressure for the development of prostate cancer that is resistance to hormone-deprivation therapies. Furthermore, our study provides a compendium of 57 ChIP-Seq experiments of key transcription factors and histone modifications in prostate cancer, which will be invaluable for prostate cancer and steroid hormone research.

EXPERIMENTAL PROCEDURES

Cell Culture and In Vitro Overexpression, Inhibition, and Function Assays

LNCaP, VCaP, RWPE, and 22RV1 cell lines were obtained from ATCC and cultured accordingly. Adenoviral and lentiviral constructs expressing ERG or GUS control were generated as previously described by recombining pCR8-ERG and a control entry clone (pENTR-GUS) (Invitrogen) with pAD/CMV/V5 and pLenti6/CMV/V5, respectively, using LR Clonase II (Invitrogen) (Tomlins et al., 2008). The pENTR-GUS serves as a positive control for the LR recombination reaction and GUS refers to beta-Glucuronidase, a protein detectable by either a fluorescent or blue substrate in the cells. VCaP cells were infected with ERG or GUS lentiviruses, and stable clones expressing ERG (VCaP+ERG) or GUS (VCaP+GUS) were selected.

For RNA interference, cells were treated with non-targeting siRNA (D-001210-01), or siRNA specific to ERG (D-003886-01) or AR (J-003400) from Dharmacon. For androgen treatment, cells were hormone starved for

2 to 3 days before treated with 1 nM R1881 for 48 hr (for expression assay) or 10 nM R1881 for 16 hr (for ChIP). Cell proliferation and invasion assays were carried out as previously described (Yu et al., 2007a).

ChIP and ChIP-Seq Assays

ChIP was carried out as previously described (Yu et al., 2007a) and detailed in the Supplemental Information. Antibodies used include AR (no. 06-680), H3K27me3 (no. 07-449), and Ace-H3 (no. 06-599) from Millipore; ERG (SC354X, Santa Cruz); and H3K4me3 (ab8580), H3K9me3 (ab8898), H3K4me1 (ab8895), H3K4me2 (ab7766), H3K36me3 (ab9050), Pan-H3 (ab1791), FoxA1 (ab23738), and RNA PolII (ab817) from Abcam. ChIP DNA was prepared into libraries and sequenced using the Genome Analyzer (Illumina) following manufacturer's protocols. The raw sequencing image data were analyzed by the Illumina analysis pipeline, aligned to the unmasked human reference genome (NCBI v36, hg18) using ELAND (Illumina), which is further analyzed by HPeak (<http://www.sph.umich.edu/csg/qin/HPeak/> and Supplemental Information) to identify enriched peak regions.

Quantitative RT-PCR

Quantitative RT-PCR was performed using Power SYBR Green Mastermix (Applied Biosystems) on an Applied Biosystems 7300 Real Time PCR machine as previously described (Yu et al., 2007a). All primers (listed in Supplemental Information) were designed using Primer 3 and synthesized by Integrated DNA Technologies.

In Vitro Protein Interaction Assay

ERG and its subdomains were cloned into pFN19A (HaloTag) vector (Promega, Madison, WI) and expressed in TNT® SP6 High-Yield Wheat Germ Reaction. A total of 2.0 μ l cell-free reaction containing the HaloTag fusion protein was mixed with 8 μ l HaloTag® Biotin Ligand (final concentration 1 μ M), and incubated at room temperature (RT) for 30 min. The biotin-labeled samples were separated on SDS gel and blotted using HRP-streptavidin to confirm HaloTag fusion protein expression. In vitro pull-down assay AR protein fragments containing the DNA-binding and ligand-binding domains were expressed in bacteria with GST-tag at N-terminal and purified by glutathione beads. A total of 12.5 μ l cell-free reaction containing HaloTag fusion proteins were incubated with 100 ng GST-AR proteins in PBST (0.1% Tween) at 4°C overnight. Ten microliter HaloLink beads (Promega) were blocked in BSA at 4°C overnight. After three washes with phosphate-buffered saline, the beads were mixed with Halo-ERG and incubated at RT for 1 hr. HaloLink beads were then washed with PBST for four times and eluted in SDS loading buffer. Proteins were separated on SDS gel and blotted with anti-GST mAb (Sigma) to detect AR. Bare HaloLink beads without HaloTag fusion proteins were used as negative controls.

Luciferase Reporter Assay

Luciferase reporter assays were performed as previously described (Cao et al., 2008). Briefly, LNCaP cells were infected with ERG or LacZ adenovirus. At 24 hr postinfection promoter-reporter constructs were cotransfected along with pRL-TK (internal control). Cells were lysed with passive lysis buffer and luciferase activities were monitored using dual luciferase assay system (Promega) after an additional 24 hr of incubation. Reporter constructs, pGL3-CDH1-Luc, pGL3 PSA6.0-Luc, and pGL3-ALP-Luc were provided by Drs. Eric Fearon (Hajra et al., 1999), Evan T. Keller (Mizokami et al., 2000), and Mitsutoki Hatta (Hatta et al., 2002), respectively. *TMPRSS2* (chr21:41,801,764-41,802,692) and AR (chrX:66,679,691-66,680,682) promoters were PCR amplified and subcloned into pGL4.14 vector (Promega) using BglII and HindIII enzymes.

Bioinformatics Analysis

Predefined motifs of transcription factors were searched using MatInspector (Cartharius et al., 2005) (Genomatix). Overrepresentation of a motif in ChIP-Seq binding sites was evaluated against control sequences randomly collected from regions other than binding sites and the significance tested by Fisher's exact test. De novo motif was analyzed using MEME (Bailey and Elkan, 1994). GSEA analysis was performed as detailed in the Supplemental Information. MCM was performed using a query gene list to search for all concepts available in the Oncomine database as previously described (Yu et al., 2007b). Concepts with significant enrichment by the query concept

were exported into a table (see Table S4). Representative concepts were selectively shown as a network in a figure (see Figure 1C).

ACCESSION NUMBERS

The microarray and short-read sequencing data have been deposited in the National Center for Biotechnology Information Gene Expression Omnibus and Short-Read Archive with the accession number GSE14097.

SUPPLEMENTAL INFORMATION

Supplemental Information includes six figures, five tables, and Supplemental Experimental Procedures and can be found with this article online at doi: 10.1016/j.ccr.2010.03.018.

ACKNOWLEDGMENTS

We thank R. Mehra and B. Han for histopathologic assessment of tissue and J. Shen, S. Kalyana-Sundaram, and A. Sreekumar for technical assistance. A.M.C. is supported by a Burroughs Wellcome Foundation Award in Clinical Translational Research, a Doris Duke Charitable Foundation Distinguished Clinical Investigator Award, and the Howard Hughes Medical Institute. A.M.C. is an American Cancer Society Research Professor. This work was supported in part by the NIH Prostate Specialized Program of Research Excellence grant P50CA69568, Early Detection Research Network grant UO1 111275 (to A.M.C.), 1R01CA132874-01A1 (to A.M.C.), K99CA129565-01A1 (to J.Y.), 1R01HG005119 (to Z.Q.), P50CA090386, the Prostate Cancer Foundation (to A.M.C.), and the U.S. Department of Defense PC051081 (to A.M.C. and S.V.), and PC080665 (to J.Y.). The University of Michigan has filed for a patent on the detection of ETS gene fusions in prostate cancer, on which S.T. and A.C. are listed as coinventors. The University of Michigan licensed the diagnostic field of use of the gene fusions to Gen-Probe, Inc. S.T. has served as a consultant to Cougar Biotechnology. A.C. has served as a consultant for Gen-Probe. Gen-Probe did not play a role in the design and conduct of this study; in the collection, analysis, or interpretation of the data; or in the preparation, review, or approval of the article.

Received: October 19, 2009

Revised: February 22, 2010

Accepted: March 31, 2010

Published: May 17, 2010

REFERENCES

- Anderson, J. (2003). The role of antiandrogen monotherapy in the treatment of prostate cancer. *BJU Int.* 91, 455–461.
- Bailey, T.L., and Elkan, C. (1994). Fitting a mixture model by expectation maximization to discover motifs in biopolymers. *Proc. Int. Conf. Intell. Syst. Mol. Biol.* 2, 28–36.
- Barski, A., Cuddapah, S., Cui, K., Roh, T.Y., Schones, D.E., Wang, Z., Wei, G., Chepelev, I., and Zhao, K. (2007). High-resolution profiling of histone methylations in the human genome. *Cell* 129, 823–837.
- Ben-Porath, I., Thomson, M.W., Carey, V.J., Ge, R., Bell, G.W., Regev, A., and Weinberg, R.A. (2008). An embryonic stem cell-like gene expression signature in poorly differentiated aggressive human tumors. *Nat. Genet.* 40, 499–507.
- Boyer, L.A., Plath, K., Zeitlinger, J., Brambrink, T., Medeiros, L.A., Lee, T.I., Levine, S.S., Wernig, M., Tajonar, A., Ray, M.K., et al. (2006). Polycomb complexes repress developmental regulators in murine embryonic stem cells. *Nature* 441, 349–353.
- Cao, Q., Yu, J., Dhanasekaran, S.M., Kim, J.H., Mani, R.S., Tomlins, S.A., Mehra, R., Laxman, B., Cao, X., Yu, J., et al. (2008). Repression of E-cadherin by the polycomb group protein EZH2 in cancer. *Oncogene* 27, 7274–7284.
- Cartharius, K., Frech, K., Grote, K., Klocke, B., Haltmeier, M., Klingenhoff, A., Frisch, M., Bayerlein, M., and Werner, T. (2005). MatInspector and beyond: promoter analysis based on transcription factor binding sites. *Bioinformatics* 21, 2933–2942.
- Carver, B.S., Tran, J., Chen, Z., Carracedo-Perez, A., Alimonti, A., Nardella, C., Gopalan, A., Scardino, P.T., Cordon-Cardo, C., Gerald, W., and Pandolfi, P.P. (2009). ETS rearrangements and prostate cancer initiation. *Nature* 457, E1, 2–3.
- Chen, H., Tu, S.W., and Hsieh, J.T. (2005). Down-regulation of human DAB2IP gene expression mediated by polycomb Ezh2 complex and histone deacetylase in prostate cancer. *J. Biol. Chem.* 280, 22437–22444.
- Clark, J., Merson, S., Jhavar, S., Flohr, P., Edwards, S., Foster, C.S., Eeles, R., Martin, F.L., Phillips, D.H., Crundwell, M., et al. (2007). Diversity of TMPRSS2-ERG fusion transcripts in the human prostate. *Oncogene* 26, 2667–2673.
- Hajra, K.M., Ji, X., and Fearon, E.R. (1999). Extinction of E-cadherin expression in breast cancer via a dominant repression pathway acting on proximal promoter elements. *Oncogene* 18, 7274–7279.
- Hatta, M., Daitoku, H., Matsuzaki, H., Deyama, Y., Yoshimura, Y., Suzuki, K., Matsumoto, A., and Fukamizu, A. (2002). Regulation of alkaline phosphatase promoter activity by forkhead transcription factor FKHR. *Int. J. Mol. Med.* 9, 147–152.
- Heemers, H.V., and Tindall, D.J. (2007). Androgen receptor (AR) coregulators: a diversity of functions converging on and regulating the AR transcriptional complex. *Endocr. Rev.* 28, 778–808.
- Hermans, K.G., van Marion, R., van Dekken, H., Jenster, G., van Weerden, W.M., and Trapman, J. (2006). TMPRSS2:ERG fusion by translocation or interstitial deletion is highly relevant in androgen-dependent prostate cancer, but is bypassed in late-stage androgen receptor-negative prostate cancer. *Cancer Res.* 66, 10658–10663.
- Hsu, T., Trojanowska, M., and Watson, D.K. (2004). Ets proteins in biological control and cancer. *J. Cell. Biochem.* 91, 896–903.
- Jia, L., Berman, B.P., Jariwala, U., Yan, X., Cogan, J.P., Walters, A., Chen, T., Buchanan, G., Frenkel, B., and Coetzee, G.A. (2008). Genomic androgen receptor-occupied regions with different functions, defined by histone acetylation, coregulators and transcriptional capacity. *PLoS ONE* 3, e3645.
- Johnson, D.S., Mortazavi, A., Myers, R.M., and Wold, B. (2007). Genome-wide mapping of in vivo protein-DNA interactions. *Science* 316, 1497–1502.
- King, J.C., Xu, J., Wongvipat, J., Hieronymus, H., Carver, B.S., Leung, D.H., Taylor, B.S., Sander, C., Cardiff, R.D., Couto, S.S., et al. (2009). Cooperativity of TMPRSS2-ERG with PI3-kinase pathway activation in prostate oncogenesis. *Nat. Genet.* 41, 524–526.
- Klezovitch, O., Risk, M., Coleman, I., Lucas, J.M., Null, M., True, L.D., Nelson, P.S., and Vasioukhin, V. (2008). A causal role for ERG in neoplastic transformation of prostate epithelium. *Proc. Natl. Acad. Sci. USA* 105, 2105–2110.
- Koivisto, P., Kononen, J., Palmberg, C., Tammela, T., Hyytinen, E., Isola, J., Trapman, J., Cleutjens, K., Noordzij, A., Visakorpi, T., and Kallioniemi, O.P. (1997). Androgen receptor gene amplification: a possible molecular mechanism for androgen deprivation therapy failure in prostate cancer. *Cancer Res.* 57, 314–319.
- Kokontis, J.M., Hay, N., and Liao, S. (1998). Progression of LNCaP prostate tumor cells during androgen deprivation: hormone-independent growth, repression of proliferation by androgen, and role for p27Kip1 in androgen-induced cell cycle arrest. *Mol. Endocrinol.* 12, 941–953.
- Lee, T.I., Jenner, R.G., Boyer, L.A., Guenther, M.G., Levine, S.S., Kumar, R.M., Chevalier, B., Johnstone, S.E., Cole, M.F., Isono, K., et al. (2006). Control of developmental regulators by Polycomb in human embryonic stem cells. *Cell* 125, 301–313.
- Lupien, M., Eeckhoutte, J., Meyer, C.A., Wang, Q., Zhang, Y., Li, W., Carroll, J.S., Liu, X.S., and Brown, M. (2008). FoxA1 translates epigenetic signatures into enhancer-driven lineage-specific transcription. *Cell* 132, 958–970.
- Massie, C.E., Adryan, B., Barbosa-Morais, N.L., Lynch, A.G., Tran, M.G., Neal, D.E., and Mills, I.G. (2007). New androgen receptor genomic targets show an interaction with the ETS1 transcription factor. *EMBO Rep.* 8, 871–878.
- Mikkelsen, T.S., Ku, M., Jaffe, D.B., Issac, B., Lieberman, E., Giannoukos, G., Alvarez, P., Brockman, W., Kim, T.K., Koche, R.P., et al. (2007). Genome-wide maps of chromatin state in pluripotent and lineage-committed cells. *Nature* 448, 553–560.

- Min, J., Zaslavsky, A., Fedele, G., McLaughlin, S.K., Reczek, E.E., De Raedt, T., Guney, I., Strohlic, D.E., Macconail, L.E., Beroukhim, R., et al. (2010). An oncogene-tumor suppressor cascade drives metastatic prostate cancer by coordinately activating Ras and nuclear factor-kappaB. *Nat. Med.* *16*, 286–294.
- Mizokami, A., Gotoh, A., Yamada, H., Keller, E.T., and Matsumoto, T. (2000). Tumor necrosis factor-alpha represses androgen sensitivity in the LNCaP prostate cancer cell line. *J. Urol.* *164*, 800–805.
- Morris, M.J., Huang, D., Kelly, W.K., Slovin, S.F., Stephenson, R.D., Eicher, C., Delacruz, A., Curley, T., Schwartz, L.H., and Scher, H.I. (2009). Phase 1 trial of high-dose exogenous testosterone in patients with castration-resistant metastatic prostate cancer. *Eur. Urol.* *56*, 237–244.
- Nye, J.A., Petersen, J.M., Gunther, C.V., Jonsen, M.D., and Graves, B.J. (1992). Interaction of murine ets-1 with GGA-binding sites establishes the ETS domain as a new DNA-binding motif. *Genes Dev.* *6*, 975–990.
- Oikawa, T., and Yamada, T. (2003). Molecular biology of the Ets family of transcription factors. *Gene* *303*, 11–34.
- Perner, S., Demichelis, F., Beroukhim, R., Schmidt, F.H., Mosquera, J.M., Setlur, S., Tchinda, J., Tomlins, S.A., Hofer, M.D., Pienta, K.G., et al. (2006). TMPRSS2:ERG fusion-associated deletions provide insight into the heterogeneity of prostate cancer. *Cancer Res.* *66*, 8337–8341.
- Scher, H.I., and Sawyers, C.L. (2005). Biology of progressive, castration-resistant prostate cancer: directed therapies targeting the androgen-receptor signaling axis. *J. Clin. Oncol.* *23*, 8253–8261.
- Shin, S., Kim, T.D., Jin, F., van Deursen, J.M., Dehm, S.M., Tindall, D.J., Grande, J.P., Munz, J.M., Vasmataz, G., and Janknecht, R. (2009). Induction of prostatic intraepithelial neoplasia and modulation of androgen receptor by ETS variant 1/ETS-related protein 81. *Cancer Res.* *69*, 8102–8110.
- Soller, M.J., Isaksson, M., Elfving, P., Soller, W., Lundgren, R., and Panagopoulos, I. (2006). Confirmation of the high frequency of the TMPRSS2/ERG fusion gene in prostate cancer. *Genes Chromosomes Cancer* *45*, 717–719.
- Sun, C., Dobi, A., Mohamed, A., Li, H., Thangapazham, R.L., Furusato, B., Shaheduzzaman, S., Tan, S.H., Vaidyanathan, G., Whitman, E., et al. (2008). TMPRSS2-ERG fusion, a common genomic alteration in prostate cancer activates C-MYC and abrogates prostate epithelial differentiation. *Oncogene* *27*, 5348–5353.
- Tomlins, S.A., Laxman, B., Dhanasekaran, S.M., Helgeson, B.E., Cao, X., Morris, D.S., Menon, A., Jing, X., Cao, Q., Han, B., et al. (2007). Distinct classes of chromosomal rearrangements create oncogenic ETS gene fusions in prostate cancer. *Nature* *448*, 595–599.
- Tomlins, S.A., Laxman, B., Varambally, S., Cao, X., Yu, J., Helgeson, B.E., Cao, Q., Prensner, J.R., Rubin, M.A., Shah, R.B., et al. (2008). Role of the TMPRSS2-ERG gene fusion in prostate cancer. *Neoplasia* *10*, 177–188.
- Tomlins, S.A., Rhodes, D.R., Perner, S., Dhanasekaran, S.M., Mehra, R., Sun, X.W., Varambally, S., Cao, X., Tchinda, J., Kuefer, R., et al. (2005). Recurrent fusion of TMPRSS2 and ETS transcription factor genes in prostate cancer. *Science* *310*, 644–648.
- Varambally, S., Dhanasekaran, S.M., Zhou, M., Barrette, T.R., Kumar-Sinha, C., Sanda, M.G., Ghosh, D., Pienta, K.J., Sewalt, R.G., Otte, A.P., et al. (2002). The polycomb group protein EZH2 is involved in progression of prostate cancer. *Nature* *419*, 624–629.
- Wang, J., Cai, Y., Yu, W., Ren, C., Spencer, D.M., and Ittmann, M. (2008). Pleiotropic biological activities of alternatively spliced TMPRSS2/ERG fusion gene transcripts. *Cancer Res.* *68*, 8516–8524.
- Wang, Q., Li, W., Liu, X.S., Carroll, J.S., Janne, O.A., Keeton, E.K., Chinnaiyan, A.M., Pienta, K.J., and Brown, M. (2007). A hierarchical network of transcription factors governs androgen receptor-dependent prostate cancer growth. *Mol. Cell* *27*, 380–392.
- Wang, Q., Li, W., Zhang, Y., Yuan, X., Xu, K., Yu, J., Chen, Z., Beroukhim, R., Wang, H., Lupien, M., et al. (2009). Androgen receptor regulates a distinct transcription program in androgen-independent prostate cancer. *Cell* *138*, 245–256.
- Wright, M.E., Tsai, M.J., and Aebersold, R. (2003). Androgen receptor represses the neuroendocrine transdifferentiation process in prostate cancer cells. *Mol. Endocrinol.* *17*, 1726–1737.
- Xie, D., Gore, C., Liu, J., Pong, R.C., Mason, R., Hao, G., Long, M., Kabbani, W., Yu, L., Zhang, H., et al. (2010). Role of DAB2IP in modulating epithelial-to-mesenchymal transition and prostate cancer metastasis. *Proc. Natl. Acad. Sci. USA* *107*, 2485–2490.
- Yoshimoto, M., Joshua, A.M., Chilton-Macneill, S., Bayani, J., Selvarajah, S., Evans, A.J., Zielenska, M., and Squire, J.A. (2006). Three-color FISH analysis of TMPRSS2/ERG fusions in prostate cancer indicates that genomic microdeletion of chromosome 21 is associated with rearrangement. *Neoplasia* *8*, 465–469.
- Yu, J., Cao, Q., Mehra, R., Laxman, B., Yu, J., Tomlins, S.A., Creighton, C.J., Dhanasekaran, S.M., Shen, R., Chen, G., et al. (2007a). Integrative genomics analysis reveals silencing of beta-adrenergic signaling by polycomb in prostate cancer. *Cancer Cell* *12*, 419–431.
- Yu, J., Rhodes, D.R., Tomlins, S.A., Cao, X., Chen, G., Mehra, R., Wang, X., Ghosh, D., Shah, R.B., Varambally, S., et al. (2007b). A polycomb repression signature in metastatic prostate cancer predicts cancer outcome. *Cancer Res.* *67*, 10657–10663.
- Zong, Y., Xin, L., Goldstein, A.S., Lawson, D.A., Teitell, M.A., and Witte, O.N. (2009). ETS family transcription factors collaborate with alternative signaling pathways to induce carcinoma from adult murine prostate cells. *Proc. Natl. Acad. Sci. USA* *106*, 12465–12470.